ELSEVIER

Journal of Molecular Structure (Theochem) 461–462 (1999) 55–69

THEO CHEM

Complete active space valence bond method applied to chemical reactions ☆

Haruyuki Nakano*, Kenichi Nakayama, Kimihiko Hirao

Department of Applied Chemistry, Graduate School of Engineering, University of Tokyo, 7-3-1 Hongo, Bunkyo-ku, Tokyo 113-8656, Japan

Received 25 May 1998; accepted 7 July 1998

Abstract

A complete active space valence bond (CASVB) method with orthogonal and non-orthogonal orbitals is applied to the collinear exchange reaction $H + H_2 \rightarrow H_2 + H$ and the unimolecular dissociation $H_2CO \rightarrow H_2 + CO$. The bond nature during the reactions is analyzed using the occupation number (weight) of the valence bond resonance structures. The CASVB descriptions with orthogonal and non-orthogonal orbitals give a similar picture, although the ratio of covalent vs. ionic bonds are quite different. In the $H_2CO \rightarrow H_2 + CO$ reaction, the CH bond dissociation and HH bond formation occur after passing through the transition state. CASVB gives a clear understanding of reaction mechanisms in terms of competing bonding schemes whose weights change along the intrinsic reaction coordinate.

Keywords: Complete active space; Valence bond method; Chemical reaction; Bond nature; Occupation number analysis

1. Introduction

To understand chemical reaction mechanisms it is crucial to obtain accurate potential energy surfaces (PESs). At present we can choose from methods at various levels, from Hartree–Fock to multireference-based techniques such as multireference configuration interaction (MRCI), multireference cluster expansion, and multireference perturbation methods for PESs. Even today, however, it is not a simple task to obtain chemical pictures at the transition state (TS) or along a reaction path. The modern electronic structure theories mentioned above certainly yield PESs with high accuracy, but their wave functions are usually so complicated that we cannot easily extract a chemical picture from the wave functions. Discussion on the nature of TS is, for instance, often conducted using other features such as molecular structures and energy profiles rather than the wave functions themselves: if the bond

☆ Dedicated to Professor Keiji Morokuma in celebration of his 65th birthday.

* Corresponding author. E-mail: nakano@qcl.t.u-tokyo.ac.jp

0166-1280/99/$ - see front matter
PII: S0166-1280(98)00462-X

length at TS is closer to that of the product than reactant, it is called a *late* TS, or if the reaction is highly exothermic, this reaction is assumed to proceed via an *early* TS. These discussions are qualitative and ambiguous. A more quantitative and clear-cut chemical description is necessary.

Recently we have proposed a complete active space valence bond (CASVB) method as a tool for interpreting the complete active space self-consistent field (CASSCF) wave function [1,2]. CASSCF is a method often used in examining potential energy surfaces of chemical reactions. In fact, this method is feasible and gives surfaces of good quality, and is also used as a starting point for higher-level multireference methods. The CASSCF method has many advantages: (1) it is well defined on the whole potential energy surface of a chemical reaction if an appropriate active space is chosen; (2) it is size-consistent; and (3) it is applicable to excited states as well as the ground state in a single framework. However, it often generates too many configurations. There is, therefore, a problem in extracting a chemical description from the lengthy CASSCF wave functions. CASVB is a solution to this problem. In the CASVB method, the CASSCF wave functions are transformed into the superposition of valence bond resonance structure, composed of atomic-like orbitals without any loss of the quality of CASSCF. The energies E_i^{CASSCF} and the densities $|\Psi_i^{\mathrm{CASSCF}}|^2$ are unchanged in the transformation.

With this method, we clarified the electronic structures of the ground and excited states of benzene, butadiene, methane, and hydrogen molecules [1,2]. We also applied the method to valence excited states of polyenes [3] and their cations [4]. In previous studies, we put our focus on the formalism of CASVB and its applicability to the molecules in the equilibrium structures. In this article, we present the application of CASVB to chemical reactions. The main purpose of the present article is to propose a quantitative measure of the chemical picture at TS and along the chemical reaction paths.

In Section 2, we briefly survey the CASVB method. We can obtain orthogonal and non-orthogonal atomic-like localized orbitals by applying Boys' localization procedure [5] and Ruedenberg's

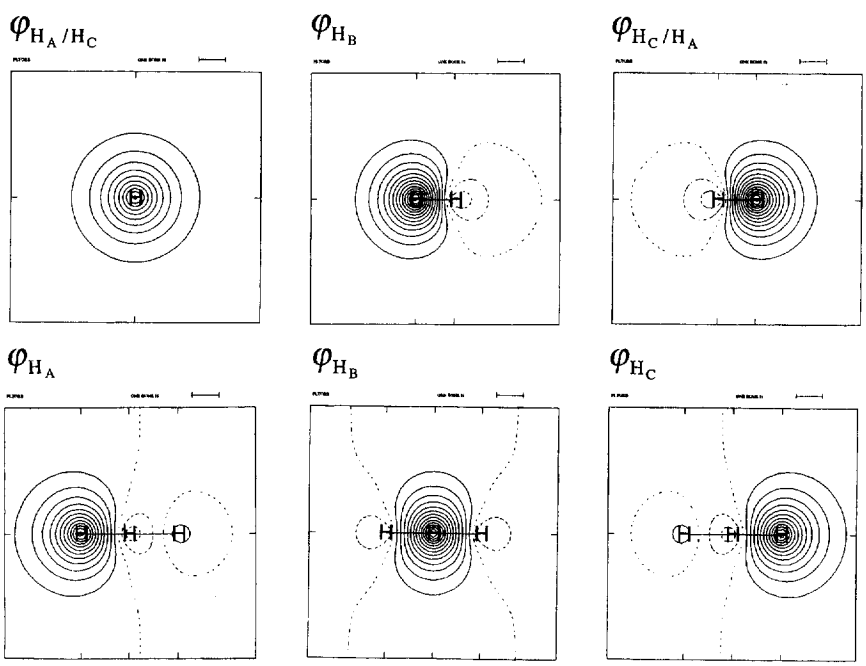

Fig. 1. Orthogonal localized orbitals of H_3 at the reactant/product and transition state structures determined with Boys' localization procedure.

projected localization method [6–8], respectively. In Section 3, the CASVB method with orthogonal and non-orthogonal localized orbitals is applied to the collinear exchange reaction $H + H_2 \rightarrow H_2 + H$ and the unimolecular dissociation $H_2CO \rightarrow H_2 + CO$, and the applicability to the reaction is discussed. Conclusions are given in Section 4.

2. Brief overview of CASVB method with orthogonal and non-orthogonal orbital sets

We have proposed two types of CASVB method [1,2]. The first one is the valence bond structures constructed from *orthogonal* localized molecular orbitals (OLMOs), and the second is the structures written with *non-orthogonal* localized molecular orbitals (NLMOs). These are henceforth referred to as OLMO-CASVB and NLMO-CASVB, respectively.

The idea of CASVB is based on the fact that the densities of variational wave functions are invariant under the transformations which hold the variational space unchanged. In the CASSCF case, a complete active space (CAS) is invariant under the linear transformation of active orbitals and also that of configuration state functions (CSFs).

We may re-define the active orbitals utilizing the invariance of the active orbital space. In the OLMO-CASVB method, the localized molecular orbitals (LMOs) constructed by Boys' localization procedure are used [5]. If the active orbitals are defined appropriately, the LMOs nearly always turn out to be localized on a single atomic center with small localization tails onto neighboring atoms. In the NLMO-CASVB case, the atomic-like orbitals are constructed by Ruedenberg's projected localization procedure [6–8].

Let Ψ^{CASSCF} be a CASSCF wave function

$$\Psi^{\mathrm{CASSCF}} = \sum_i C_i \Phi_i^{\mathrm{CSF}}, \quad \Phi_i^{\mathrm{CSF}} \equiv \Phi_i^{\mathrm{CSF}}(\{\varphi_i\}) \qquad (1)$$

where Φ_i^{CSF} are the configuration state functions constructed by the orthogonal orbitals set $\{\varphi_i\}$ and C_i are the known CAS configuration interac-

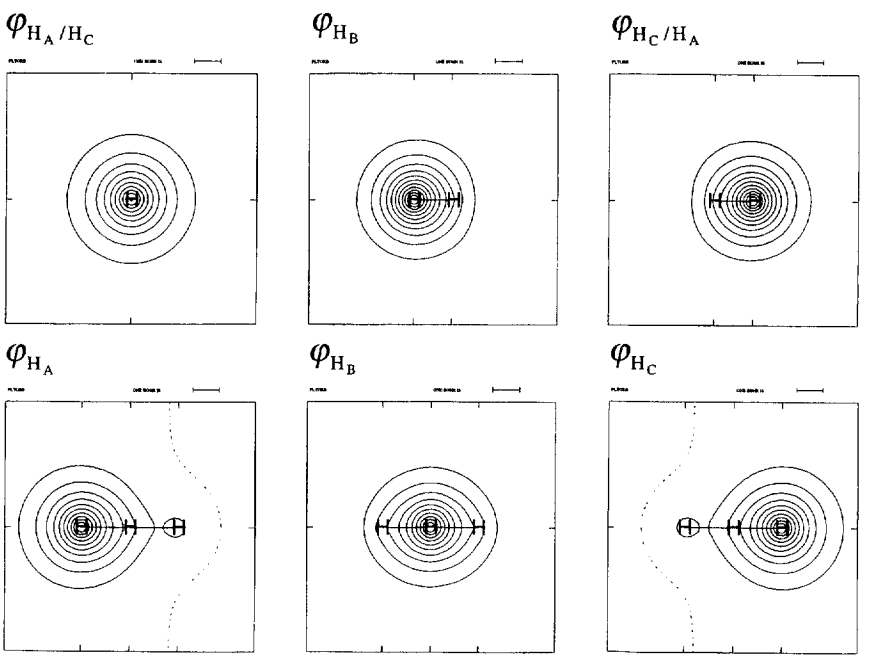

Fig. 2. Non-orthogonal localized orbitals of H_3 at the reactant/product and transition state structures determined with Ruedenberg's projected localization procedure.

tion (CI) expansion coefficients. Similarly define the CASVB function in terms of spin-paired functions as

$$\Psi^{\mathrm{CASVB}} = \sum_i A_i \Phi_i^{\mathrm{VB}}, \quad \Phi_i^{\mathrm{VB}} \equiv \Phi_i^{\mathrm{VB}}(\{\lambda_i\}) \tag{2}$$

where Φ_i^{VB} are spin-paired functions constructed by LMOs. The number of independent spin-paired functions is equal to the dimension of CAS. The spaces spanned by $\{\Phi_i^{\mathrm{CSF}}\}$ and $\{\Phi_i^{\mathrm{VB}}\}$ are identical. Since Eqs. (1) and (2) are different expressions of the identical wave function, we may write

$$\sum_j A_j \Phi_j^{\mathrm{VB}} = \sum_j C_j \Phi_j^{\mathrm{CSF}}. \tag{3}$$

Left-multiplying Eqs. (1) and (2) by Φ_i^{CSF} and integrating the products, we get

$$\sum_j \Omega_{ij} A_j = C_i \quad \text{with} \quad \Omega_{ij} = \langle \Phi_i^{\mathrm{CSF}} | \Phi_j^{\mathrm{VB}} \rangle, \tag{4}$$

whose dimension is equal to the dimension of CAS. Solving this linear equation, we obtain CASVB wave function Ψ^{CASVB}. In the OLMO-CASVB case, we can use the common set of (Boys') LMOs as $\{\varphi_i\}$ as well as $\{\lambda_i\}$ since the LMOs remain CASSCF MOs. In that case, the linear Eq. (4) reduces to a set of linear equations for each *orbital* configuration, and the matrix Ω_{ij} for each linear equation becomes a triangular matrix depending only on spin configurations. The linear Eq. (4) can, therefore, be solved with ease, compared with the NLMO-CASVB case.

The occupation number (or weight) of a resonance structure is calculated with

$$n_i = A_i^* \sum_j S_{ij} A_j, \tag{5}$$

where S_{ij} are overlaps between the structures i and j, defined by

$$S_{ij} = \langle \Phi_i^{\mathrm{VB}} | \Phi_j^{\mathrm{VB}} \rangle \tag{6}$$

and satisfies the normalization,

Table 1
Spin-paired functions and resonance structures of H_3 (normalization and phase factors are omitted)

Spin-paired function	Resonance structure	
$\varphi_{\mathrm{H_A}}\varphi_{\mathrm{H_B}}(\alpha\beta-\beta\alpha)\cdot\varphi_{\mathrm{H_C}}\alpha$	$\mathrm{H_A}$–$\mathrm{H_B}$ $\dot{\mathrm{H}}_{\mathrm{C}}$	(I)
$\varphi_{\mathrm{H_B}}\varphi_{\mathrm{H_B}}\alpha\beta\cdot\varphi_{\mathrm{H_C}}\alpha$	$\mathrm{H_A^+}$ $^-\mathrm{H_B}$ $\dot{\mathrm{H}}_{\mathrm{C}}$	(II)
$\varphi_{\mathrm{H_A}}\varphi_{\mathrm{H_A}}\alpha\beta\cdot\varphi_{\mathrm{H_C}}\alpha$	$\mathrm{H_A^-}$ $^+\mathrm{H_B}$ $\dot{\mathrm{H}}_{\mathrm{C}}$	(III)
$\varphi_{\mathrm{H_A}}\alpha\cdot\varphi_{\mathrm{H_B}}\varphi_{\mathrm{H_C}}(\alpha\beta-\beta\alpha)$	$\dot{\mathrm{H}}_{\mathrm{A}}$ $\mathrm{H_B}$–$\mathrm{H_C}$	(IV)
$\varphi_{\mathrm{H_A}}\alpha\cdot\varphi_{\mathrm{H_B}}\varphi_{\mathrm{H_B}}\alpha\beta$	$\dot{\mathrm{H}}_{\mathrm{A}}$ $\mathrm{H_B^-}$ $^+\mathrm{H_C}$	(V)
$\varphi_{\mathrm{H_A}}\alpha\cdot\varphi_{\mathrm{H_C}}\varphi_{\mathrm{H_C}}\alpha\beta$	$\dot{\mathrm{H}}_{\mathrm{A}}$ $\mathrm{H_B^+}$ $^-\mathrm{H_C}$	(VI)
$\varphi_{\mathrm{H_B}}\alpha\cdot\varphi_{\mathrm{H_C}}\varphi_{\mathrm{H_C}}\alpha\beta$	$\mathrm{H_B^+}$ $\dot{\mathrm{H}}_{\mathrm{B}}$ $^-\mathrm{H_C}$	(VII)
$\varphi_{\mathrm{H_A}}\varphi_{\mathrm{H_A}}\alpha\beta\cdot\varphi_{\mathrm{H_B}}\alpha$	$\mathrm{H_A^-}$ $\dot{\mathrm{H}}_{\mathrm{B}}$ $^+\mathrm{H_C}$	(VIII)

$$\sum_i n_i = 1. \tag{7}$$

Note that the occupation number n_i could be negative because of the non-orthogonality of resonance structures.

Thorsteinsson et al. also investigated the transformations of CASSCF functions to modern valence bond representations (they also call it CASVB) [9–11]. They examined transformations for which the total wave function is dominated by some VB structures (e.g. covalent structures) built from a common product of non-orthogonal orbitals.

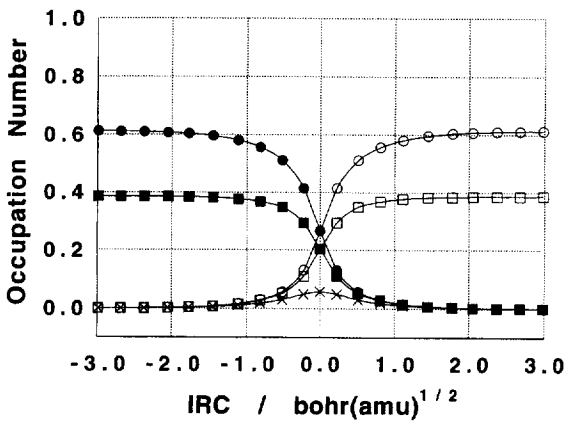

Fig. 3. Changes in the occupation numbers of the covalent H_AH_B bond (●), ionic H_AH_B bond (■), covalent H_BH_C bond (○), ionic H_BH_C bond (□), and ionic H_AH_C (×) valence bond (VB) structures of H_3 along the intrinsic reaction coordinate (IRC) in the OLMO-CASVB case. The origin of the horizontal axis corresponds to the transition state.

3. Application to chemical reactions

3.1. Collinear exchange reaction $H + H_2 \rightarrow H_2 + H$

The first example is the collinear exchange reaction $H + H_2 \rightarrow H_2 + H$, which proceeds via a symmetric transition state.

A number of potential energy surfaces have been obtained since the early works by Liu and co-workers [12–15]. Recently benchmark calculations were carried out by Peterson et al. using the multireference configuration interaction method [16]. They obtained 9.62 kcal/mol for the barrier height of the reaction, in very good agreement with the quantum Monte Carlo value, 9.60 kcal/mol [17]. A valence bond method adopting another philosophy has also been applied to the electronic structure at TS of this reaction [18,19].

To obtain a CASVB description, we first carry out a standard CASSCF calculation. The basis set used is Dunning's correlation-consistent valence-double-zeta plus polarization basis set (cc-pVDZ) [20,21]. Three electrons are distributed among three 1s orbitals of hydrogen to construct the active space. The reactant, product, and TS structure of this reaction are determined with the same method. The reactant and product structures of the H_3 supersystem are deduced from a hydrogen molecule H_2 with a bond length of 0.7705 Å and a hydrogen atom H. The HH distance is computed to be 0.9679 Å for the TS. The calculated barrier height is 16.38 kcal/mol, which is remedied to 11.08 kcal/mol by taking into account the dynamic electron correlation with second-order multireference perturbation theory [22–25]. The full CI values with the same basis set is 10.247 kcal/mol [16].

Fig. 1 shows orthogonal localized orbitals at the reactant (product) structure and TS. Fig. 2 gives non-orthogonal localized orbitals. The overlaps between the atomic orbital (AO) and non-orthogonal MO are 0.9889 on the atoms in the

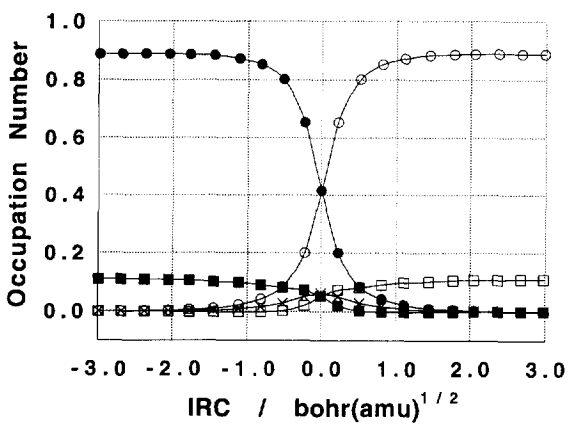

Fig. 4. Changes in the occupation numbers of the covalent H_AH_B bond (●), ionic H_AH_B bond (■), covalent H_BH_C bond (○), ionic H_BH_C bond (□), and ionic H_AH_C (×) VB structures of H_3 along the IRC in the NLMO-CASVB case.

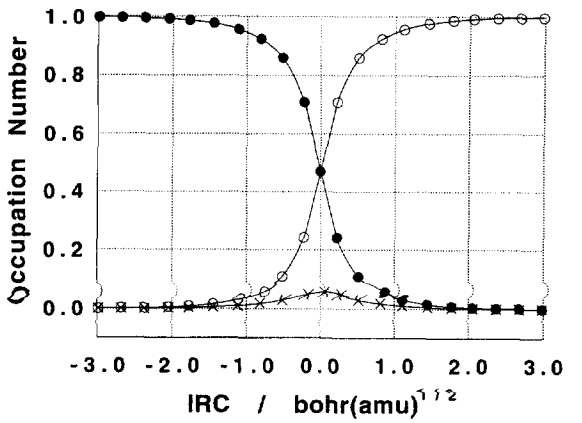

Fig. 5. Changes in the occupation numbers of the total H_AH_B bond (●), total H_BH_C bond (○), and ionic H_AH_C (×) VB structures of H_3 along the IRC in the OLMO-CASVB case.

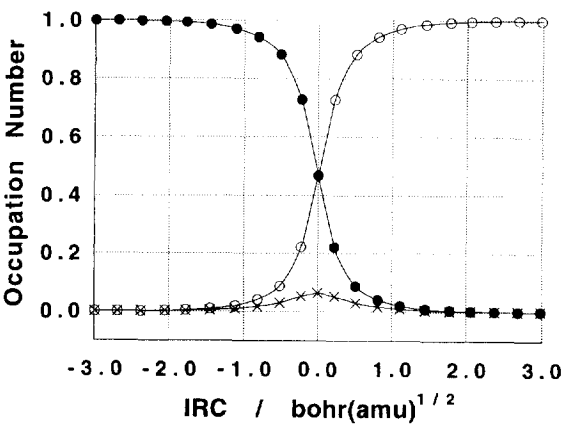

Fig. 6. Changes in the occupation numbers of the total H_AH_B bond (●), total H_BH_C bond (○), and ionic H_AH_C (×) VB structures of H_3 along the IRC in the NLMO-CASVB case.

hydrogen molecule at the reactant/product structure, and 0.9942 and 0.9938 on the central atom and the terminal atoms, respectively, at TS structure. The molecular orbitals are well localized.

There are eight spin-paired functions, corresponding to the dimension of CAS(3,3), for this system, which are listed in Table 1.

In Table 1, resonance structure (I) is a covalent structure including the H_AH_B covalent bond, and (II) and (III) are ionic structures where the H_AH_B bond is polarized. These three structures may be classified as H_AH_B bond structures. Structures (IV), (V), and (VI) are classified as H_BH_C bond structures. Structures (VII) and (VIII) may not be classified as either of the above.

Since the hydrogen molecule in its equilibrium structure is written as

$$0.6133\left[\varphi_{H_A}\varphi_{H_B}(\alpha\beta-\beta\alpha)/\sqrt{2}\right] + 0.3867[\varphi_{H_A}\varphi_{H_A}\alpha\beta+\varphi_{H_B}\varphi_{H_B}\alpha\beta] \quad (8)$$

by the OLMO-CASVB and as

$$0.8891\left[\varphi_{H_A}\varphi_{H_B}(\alpha\beta-\beta\alpha)/\sqrt{2}\right] + 0.1109[\varphi_{H_A}\varphi_{H_A}\alpha\beta+\varphi_{H_B}\varphi_{H_B}\alpha\beta] \quad (9)$$

by the NLMO-CASVB [26], the reactant (product) is written as

$$\Psi_{Reactant} = 0.6133[(I)] + 0.3867[(II) + (III)] \quad (10)$$

$$(\Psi_{Product} = 0.6133[(IV)] + 0.3867[(V) + (VI)]) \quad (11)$$

in the OLMO-CASVB case and

$$\Psi_{Reactant} = 0.8891[(I)] + 0.1109[(II) + (III)] \quad (12)$$

$$(\Psi_{Product} = 0.8891[(IV)] + 0.1109[(V) + (VI)]) \quad (13)$$

in the NLMO-CASVB case. The numbers before the structures represent the occupation numbers defined by Eq. (5). The use of non-orthogonal orbitals places a higher weight on covalent structures than when orthogonal orbitals are used.

In the TS structure, the wave function is written as

$$\Psi_{TS} = 0.5350[(I) + (IV)] + 0.2386[(II) + (V)] + 0.1690[(III) + (VI)] + 0.0574[(IV) + (VIII)] \quad (14)$$

in the OLMO-CASVB and as

$$\Psi_{TS} = 0.8316[(I) + (IV)] + 0.0935[(II) + (V)] + 0.0126[(III) + (VI)] + 0.0623[(IV) + (VIII)] \quad (15)$$

in the NLMO-CASVB. The occupation number of [(I) + (IV)] is given approximately by the average of the occupation numbers of structures (I) in the reactant and structure (IV) in the product,

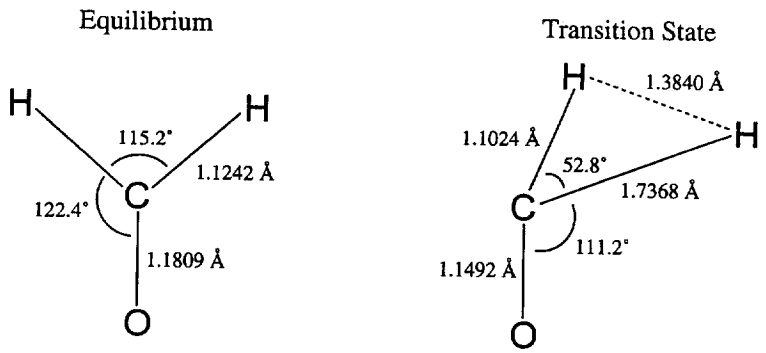

Fig. 7. The equilibrium structure of H_2CO and transition state structure of the $H_2CO \rightarrow H_2 + CO$ reaction determined with the CASSCF method (CAS(4,4)).

and similarly, the occupation number of [(II) + (V)]/[(III) + (VI)] is approximately the average of the occupation numbers of structures (II)/(III) in the reactant and (V)/(VI) in the product. In other words, TS is roughly described by the average of the reactant and product. Thus, the tendency of the resonance structures in the equilibrium structure is true of those in the TS: the covalent structures are still dominant although the ratio of covalent to ionic structures decreases a little. Of two types of ionic structure (the structures (II) and (V) where one terminal H is positive and the structures (III) and (VI) where one terminal H is negative), the former type contributes slightly more than the latter. Mulliken population analysis also shows that the central atom is slightly negative: −0.02.

Fig. 3 shows the changes in the occupation numbers of the competing bonds along the intrinsic reaction coordinate (IRC) in the OLMO-CASVB case. The covalent H_AH_B bond, ionic H_AH_B bond, covalent H_BH_C bond, ionic H_BH_C bond, and ionic H_AH_C valence bond (VB) structures of H_3 are defined by

$$n_{\text{Covalent } H_AH_B} = n_{\text{I}}, \quad n_{\text{Ionic } H_AH_B} = n_{\text{II}} + n_{\text{III}}, \tag{16}$$

$$n_{\text{Covalent } H_BH_C} = n_{\text{IV}}, \quad n_{\text{Ionic } H_BH_C} = n_{\text{V}} + n_{\text{VI}}, \tag{17}$$

and

$$n_{\text{Ionic } H_AH_C} = n_{\text{VII}} + n_{\text{VIII}}. \tag{18}$$

This figure indicates that the main covalent structures (I) and (IV) interchange rapidly. This is true for the ionic structures generated from (I) (i.e. (II) and (III)) and (IV) (i.e. (V) and (VI)). The contributions from the ionic bond between terminal H_A and H_C remain small over the entire path.

Fig. 4 presents the changes in the occupation numbers in the NLMO-CASVB case. We can

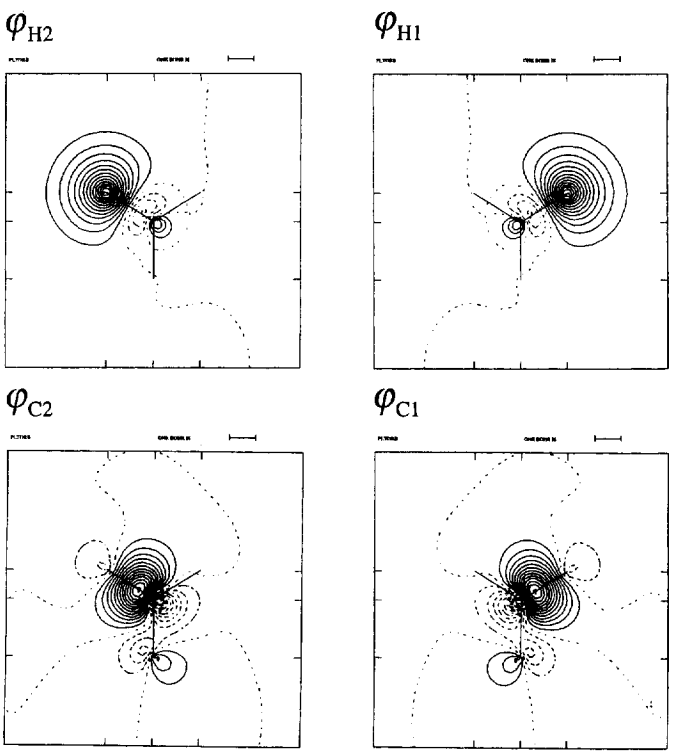

Fig. 8. The orthogonal localized orbitals at the equilibrium structure of H_2CO determined with Boys' localization procedure.

observe the same tendency, although the contribution from the ionic structures is smaller compared to the orthogonal case (< 0.12 on the whole path). Note that the ionic occupation number is the sum of two occupation numbers. Each one is less than 0.07.

Figs. 5 and 6 describe the changes in the total H_AH_B and H_BH_C bond structures, which are defined by the sums of the covalent structure (II)/(IV) and ionic structures (II)/(V) and (III)/(VI), respectively:

$$n_{H_AH_B} = n_{\text{Covalent } H_AH_B} + n_{\text{Ionic } H_AH_B},$$
$$n_{H_BH_C} = n_{\text{Covalent } H_BH_C} + n_{\text{Ionic } H_BH_C}. \quad (19)$$

Both the orthogonal and NLMO-CASVB give a quite similar picture, although the ratio of the covalent and ionic contributions are quite different. Similar to Figs. 3 and 4, the two occupation numbers interchange rapidly in the TS region, indicating the occurrence of the rapid H_AH_B bond breaking and H_BH_C bond formation in the region.

This implies that the occupation number defined by Eq. (19) can be used as an index measuring the quantity of chemical bonds during chemical reactions. It is useful in order to discuss the bond nature in the middle of a reaction, for instance in TS.

3.2. Unimolecular dissociation reaction $H_2CO \rightarrow H_2 + CO$

The next example is the dissociation reaction of formaldehyde into a hydrogen molecule and carbon monoxide. Morokuma first studied this reaction theoretically and stressed the necessity of multireference treatment [27,28]. There have been many subsequent theoretical studies on this system [29–35].

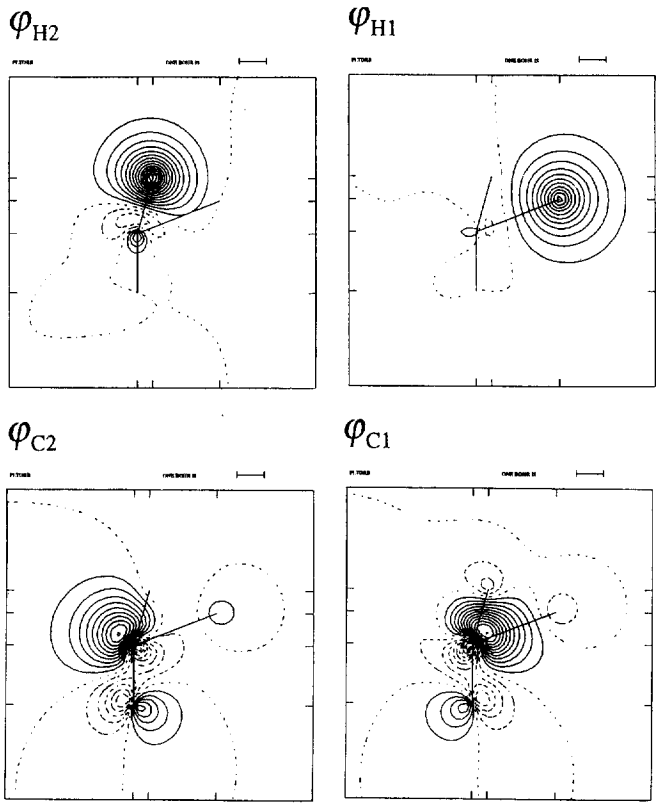

Fig. 9. The orthogonal localized orbitals at the transition state structure of the $H_2CO \rightarrow H_2 + CO$ reaction.

This reaction is Woodward–Hoffmann forbidden and proceeds via a highly asymmetric TS structure. Qualitative chemical considerations based on a correlation diagram connecting H_2CO to dissociating products have been given by Dupuis et al. [34]. Diabatically H_2CO ($^1A_1$) dissociates to H_2 ($^1\Sigma_g^+$) + CO ($^1\Pi$), while H_2 ($^1\Sigma_g^+$) and CO ($^1\Sigma^+$) interact repulsively and correlate with an excited state of H_2CO. An avoided-crossing of these two diabatic potential surfaces gives rise to a barrier for dissociation on the adiabatic ground state potential surface.

A qualitatively correct description of the dissociation process requires at least four active electrons in the two CH bonds of H_2CO. During the dissociation process, two electrons, one from each CH bond, pair up to form the HH bond while the other two form a lone pair on C in CO.

The CASSCF wave function was obtained with CAS(4,4). The basis set used is Dunning's cc-pVDZ. Six d-orbital components were used for the polarization functions of the carbon and oxygen atoms. The optimized equilibrium structure and the TS are summarized in Fig. 7. The (classical) barrier height is computed to be 90.96 kcal/mol. This is improved further by taking into account dynamic correlation with the second-order multireference perturbation theory, as shown in a previous publication [35].

The orbitals were then localized in the active orbital space. In the NLMO-CASVB case the orbitals were transformed so as to have maximum overlap with two carbon sp^2 orbitals and 1s orbitals of the hydrogen atoms. The sp^2 orbitals were used with the fixed hybridization ratio of 2s to 2p orbitals (1:2) and with a fixed angle of 120° relative to the CO axis throughout the reaction. So obtained orbitals are shown in Figs. 8–11. The

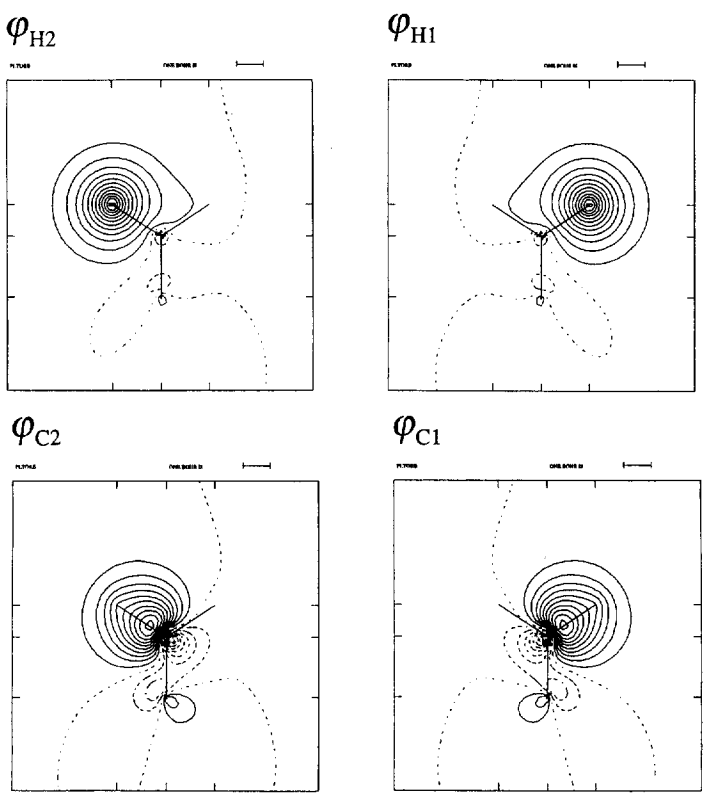

Fig. 10. The non-orthogonal localized orbitals at the equilibrium structure of H_2CO determined with Ruedenberg's projected localization procedure.

overlaps between the atomic orbitals and the obtained localized orbitals in the non-orthogonal case are

$$\langle \mathrm{AO}(\mathrm{sp}^2)|\mathrm{LMO}(\mathrm{sp}^2)\rangle = 0.9426, \quad \langle \mathrm{AO}(\mathrm{H})|\mathrm{LMO}(\mathrm{H})\rangle = 0.9710 \tag{20}$$

at the equilibrium structure and

$$\langle \mathrm{AO}(\mathrm{sp}_1^2)|\mathrm{LMO}(\mathrm{sp}_1^2)\rangle = 0.9050, \quad \langle \mathrm{AO}(\mathrm{sp}_2^2)|\mathrm{LMO}(\mathrm{sp}_2^2)\rangle = 0.8836 \tag{21}$$

$$\langle \mathrm{AO}(\mathrm{H}_1)|\mathrm{LMO}(\mathrm{H}_1)\rangle = 0.9868, \quad \langle \mathrm{AO}(\mathrm{H}_2)|\mathrm{LMO}(\mathrm{H}_2)\rangle = 0.9635 \tag{22}$$

at the TS. In all cases, the orbitals are well localized on the atomic centers, except LMOs on the carbon atom, which have a small contribution from the oxygen 2p orbital. The LMOs in the OLMO-CASVB case are quite similar in shape to the non-orthogonal LMOs.

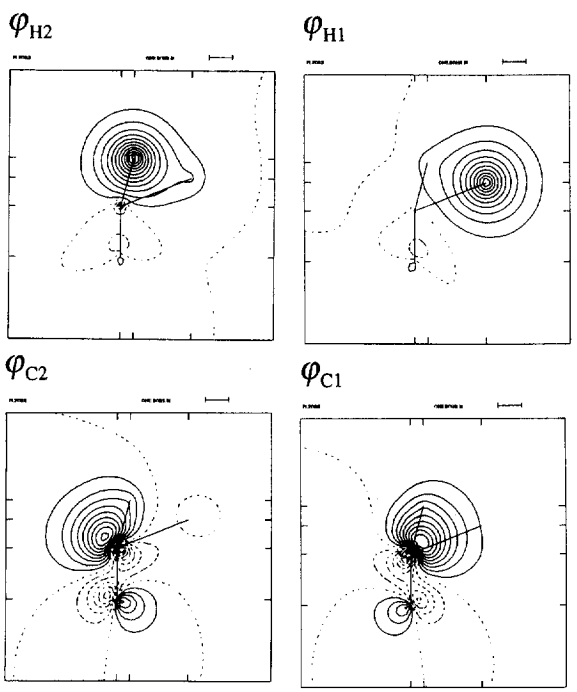

Fig. 11. The non-orthogonal localized orbitals at the transition state structure of the $H_2CO \rightarrow H_2 + CO$ reaction.

There are 20 linearly independent spin-paired functions corresponding to the dimension of CAS(4,4), which are listed in Table 2. Structures (I) to (VII) are classified as CH bond structures and the structures (VIII) to (X) as HH bond structures. Structure (XI) is classified as neither of the above, since these structures can be regarded both as structures polarized further from one of (II) to (V) and (IX) to (X).

The OLMO-CASVB wave functions obtained for the equilibrium and TS structures are given in Fig. 12.

In the equilibrium structure, the main resonance structure is the covalent CH bonds structure (I) as expected. The second most important are those where one of the CH bonds is connected with a covalent bond and the other with an ionic bond made by electron transfer from the hydrogen atom to the carbon atom, (II) and (IV). The third most important structures are (III) and (V), where one CH bond is polarized by electron transfer from the carbon atom to a hydrogen atom. The difference between the second group, (II) and (IV), and the third group, (III) and (V), is not so large, which is in good agreement with the electronegativity of H and C (2.1 and 2.5 according to Pauling's definition). The contribution from the HH bond structure (VIII) and ionic structures, (IX) and (X), is very small. The total occupation number of CH bonds is 0.8786, while that of HH bond is 0.0244. This indicates almost no bond formation between two hydrogen atoms in the equilibrium structure.

In the TS structure, the main structure is still the covalent structure (I), although the occupation number decreases. The structures (II) and (III), where the longer CH bond is covalent and the shorter CH bond is ionic, are also important, but their occupation numbers also decrease. On the other hand, the structures where the shorter CH bond is covalent and the longer CH bond is ionic, (IV) and (V), are no longer important. The total occupation number of CH bond structures is 0.6994, which shows a decrease from the value in the equilibrium structure 0.8786, but is still large. The total occupation number of HH bond structures is 0.2370. Much of it comes from the cova-

Table 2
Spin-paired functions and resonance structures of formaldehyde (normalization and phase factors are omitted)

Spin-paired function	Resonance structure	
$\varphi_{H2}\varphi_{C2}(\alpha\beta-\beta\alpha)\cdot\varphi_{C1}\varphi_{H1}(\alpha\beta-\beta\alpha)$	H_2–C–H_1	(I)
$\varphi_{C2}\varphi_{C2}\alpha\beta\cdot\varphi_{C1}\varphi_{H1}(\alpha\beta-\beta\alpha)$ $\varphi_{C1}\varphi_{C1}\alpha\beta\cdot\varphi_{C2}\varphi_{H1}(\alpha\beta-\beta\alpha)$	$H_2^{+}\ {}^{-}$C–H_1	(II)
$\varphi_{H2}\varphi_{H2}\alpha\beta\cdot\varphi_{C1}\varphi_{H1}(\alpha\beta-\beta\alpha)$ $\varphi_{H2}\varphi_{H2}\alpha\beta\cdot\varphi_{C2}\varphi_{H1}(\alpha\beta-\beta\alpha)$	$H_2^{-}\ {}^{+}$C–H_1	(III)
$\varphi_{H2}\varphi_{C2}(\alpha\beta-\beta\alpha)\cdot\varphi_{C1}\varphi_{C1}\alpha\beta$ $\varphi_{H2}\varphi_{C1}(\alpha\beta-\beta\alpha)\cdot\varphi_{C2}\varphi_{C2}\alpha\beta$	H_2–$C^{-}\ {}^{+}H_1$	(IV)
$\varphi_{H2}\varphi_{C2}(\alpha\beta-\beta\alpha)\cdot\varphi_{H1}\varphi_{H1}\alpha\beta$ $\varphi_{H2}\varphi_{C1}(\alpha\beta-\beta\alpha)\cdot\varphi_{H1}\varphi_{H1}\alpha\beta$	H_2–$C^{+}\ {}^{-}H_1$	(V)
$\varphi_{C2}\varphi_{C2}\alpha\beta\cdot\varphi_{C1}\varphi_{C1}\alpha\beta$	$H_2^{+}\ {}^{-}C^{-}\ {}^{+}H_1$	(VI)
$\varphi_{H2}\varphi_{H2}\alpha\beta\cdot\varphi_{H1}\varphi_{H1}\alpha\beta$	$H_2^{-}\ {}^{+}C^{+}\ {}^{-}H_1$	(VII)
$\varphi_{H2}\varphi_{H1}(\alpha\beta-\beta\alpha)\cdot\varphi_{C2}\varphi_{C2}\alpha\beta$ $\varphi_{H2}\varphi_{H1}(\alpha\beta-\beta\alpha)\cdot\varphi_{C2}\varphi_{C1}(\alpha\beta-\beta\alpha)$ $\varphi_{H2}\varphi_{H1}(\alpha\beta-\beta\alpha)\cdot\varphi_{C1}\varphi_{C1}\alpha\beta$	$\overline{H_2\,C\,H_1}$	(VIII)
$\varphi_{H1}\varphi_{H1}\alpha\beta\cdot\varphi_{C2}\varphi_{C1}(\alpha\beta-\beta\alpha)$	$H_2^{+}\ C\ {}^{-}H_1$	(IX)
$\varphi_{H2}\varphi_{H2}\alpha\beta\cdot\varphi_{C2}\varphi_{C1}(\alpha\beta-\beta\alpha)$	$H_2^{-}\ C\ {}^{+}C_1$	(X)
$\varphi_{H2}\varphi_{H2}\alpha\beta\cdot\varphi_{C2}\varphi_{C2}\alpha\beta$ $\varphi_{H2}\varphi_{H2}\alpha\beta\cdot\varphi_{C1}\varphi_{C1}\alpha\beta$ $\varphi_{C2}\varphi_{C2}\alpha\beta\cdot\varphi_{H1}\varphi_{H1}\alpha\beta$ $\varphi_{C1}\varphi_{H2}\alpha\beta\cdot\varphi_{H1}\varphi_{H1}\alpha\beta$	The other (doubly polarized) structures	(XI)

lent contribution (VIII), 0.1692. The contribution from the CH bonds overwhelms the contribution from the HH bond in TS.

The NLMO-CASVB wave functions in the equilibrium and transition state structures are also given in Fig. 12.

The same tendency can be seen in these wave functions except that some ionic structures have negative occupation numbers. The NLMO-CASVB also shows that there is almost no HH bond in the equilibrium structure and that the contribution from the CH bonds is dominant in TS.

Fig. 13 shows the changes in the occupation numbers of the covalent CH bonds, ionic CH bonds, covalent HH bond, ionic HH bond, and the other (doubly ionic) structures along IRC in the OLMO-CASVB case. These are defined by

$$n_{\text{Covalent CH}} = n_1, \quad n_{\text{Ionic CH}} = \sum_{S=II}^{VII} n_S, \tag{28}$$

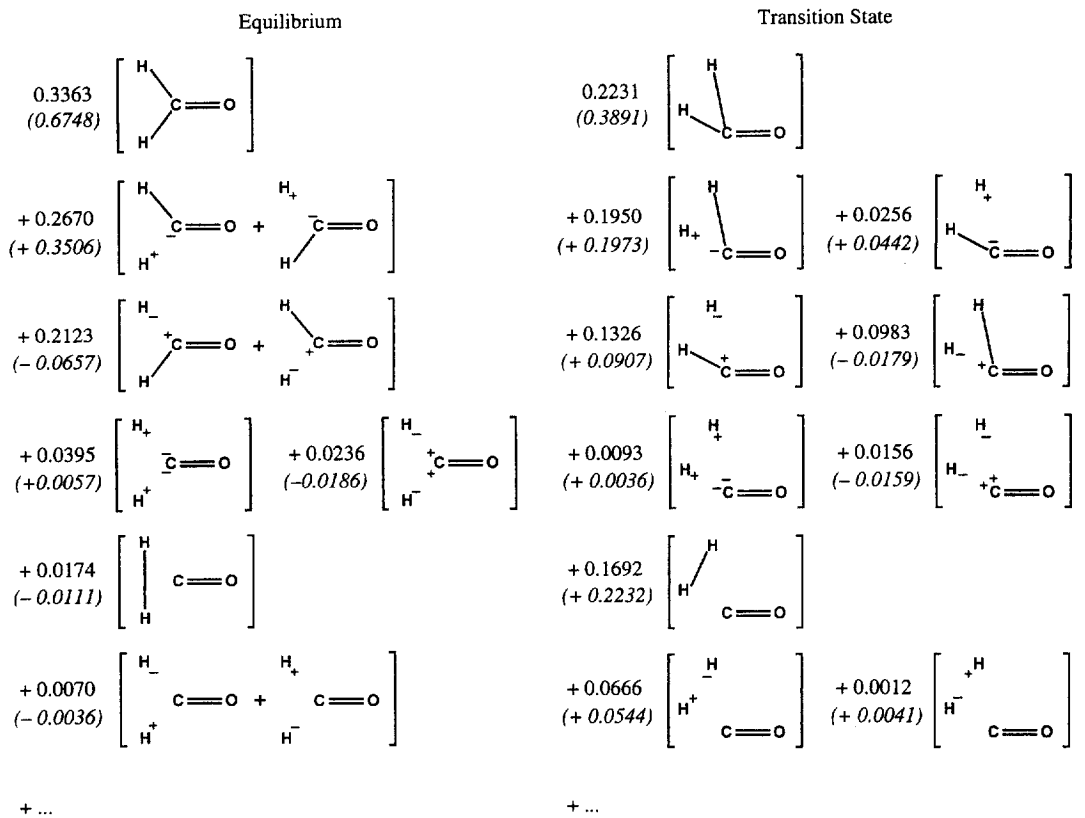

Fig. 12. The orthogonal and NLMO-CASVB descriptions at the equilibrium and transition state structures. Values before the valence bond structures are occupation numbers of OLMO-CASVB method and the values in the parentheses are those of the NLMO-CASVB method.

$$n_{\text{Covalent HH}} = n_{\text{VIII}}, \quad n_{\text{Ionic HH}} = n_{\text{IX}} + n_{\text{X}}, \tag{29}$$

and

$$n_{\text{Doubly Pol.}} = n_{\text{XI}}. \tag{30}$$

The origin of the horizontal axis corresponds to TS and the left end of each curve to the equilibrium structure. The IRC was not followed to the product $H_2 + CO$, since CAS(4,4) is not appropriate near the product. The occupation numbers of CH and HH covalent bond structures change rapidly near TS and the curves cross immediately after TS (0.1 bohr(amu)$^{1/2}$), while the occupation numbers of CH and HH ionic bond structures change slowly.

Fig. 14 illustrates the changes in the occupation numbers in the NLMO-CASVB case.

Figs. 15 and 16 show the changes in the total occupation numbers of the CH and HH bond structures along the IRC,

$$n_{\text{CH}} = n_{\text{Covalent CH}} + n_{\text{Ionic CH}},$$
$$n_{\text{HH}} = n_{\text{Covalent HH}} + n_{\text{Ionic HH}}. \tag{31}$$

It is noted that these two graphs are similar to each other, although the components of occupation numbers are rather different. In particular, near the transition state, the two cases are quite similar.

The crossing point is located after TS, 0.42 bohr(amu)$^{1/2}$ in both graphs. The structure at this point is given in Fig. 17. Compared to the TS, the longer and shorter CH bonds have stretched by 0.14 and 0.06 Å, respectively, and the HH bond has become short by 0.18 Å. These bond

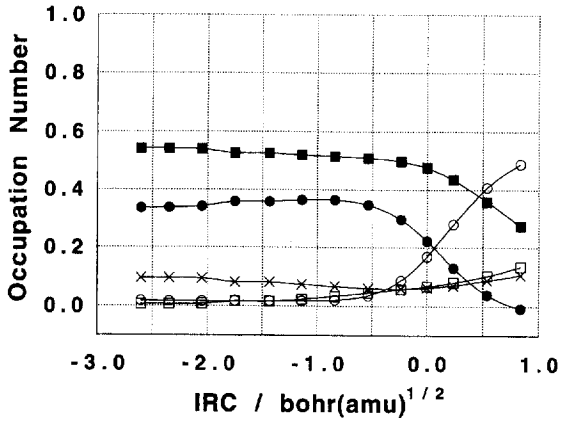

Fig. 13. Changes in the occupation numbers of the covalent CH bonds (●), ionic CH bonds (■), covalent HH bond (○), ionic HH bond (□), and the other (doubly ionic) (×) valence bond (VB) structures of H_2CO along the intrinsic reaction coordinate (IRC) in the OLMO-CASVB case. The origin of the horizontal axis corresponds to the transition state and the left end to the equilibrium structure of formaldehyde.

lengths are 1.03, 1.62, and 1.80 times longer than the corresponding equilibrium CH and HH bond distances. That point is the structure where the bonds switch; in other words, the point is the *transition state* between the CH bonds and HH bond.

The results here also demonstrate the total occupation number defined in Eq. (31) is a useful

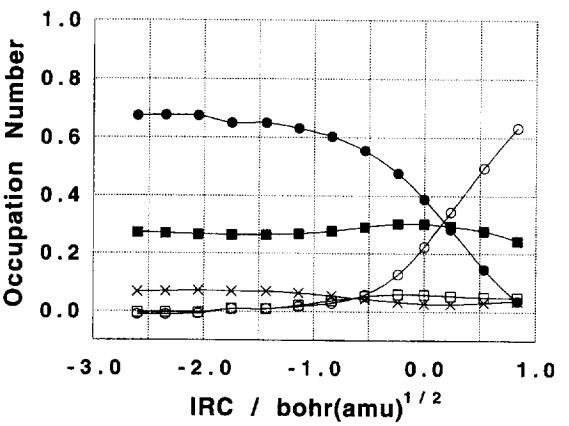

Fig. 14. Changes in the occupation numbers of the covalent CH bonds (●), ionic CH bonds (■), covalent HH bond (○), ionic HH bond (□), and the other (doubly ionic) (×) VB structures of H_2CO along IRC in the NLMO-CASVB case.

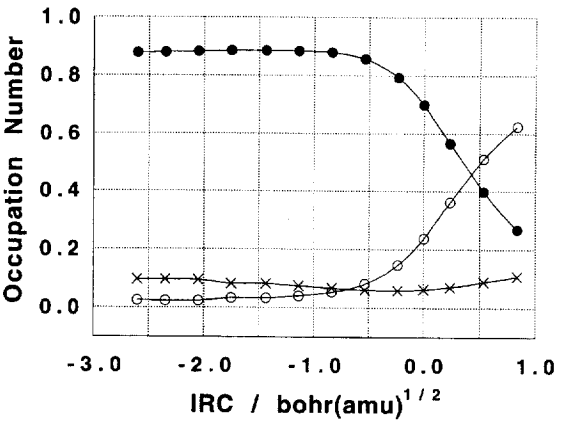

Fig. 15. Changes in the occupation numbers of the total CH bonds (●), total HH bond (○), and the other (doubly ionic) (×) VB structures of H_2CO along the IRC in the OLMO-CASVB case.

concept for studying quantitative description of chemical bonds at TS and along reaction paths.

4. Conclusions

In the present article, we investigated the nature of bonds at transition states and during chemical reactions using OLMO- and NLMO-CASVB methods. First we examined the collinear $H + H_2 \rightarrow H_2 + H$ reaction. The total occupation

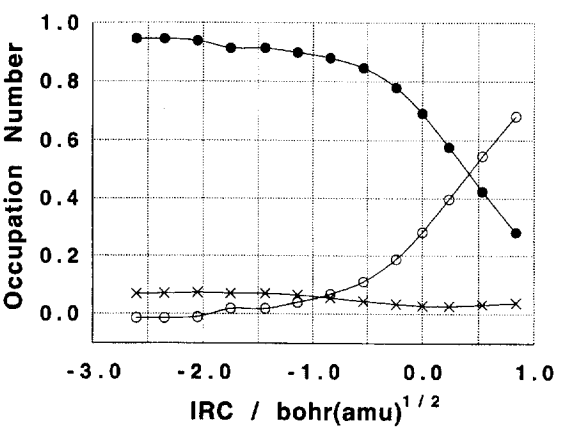

Fig. 16. Changes in the occupation numbers of the total CH bonds (●), total HH bond (○), and the other (doubly ionic) (×) VB structures of H_2CO along the IRC in the NLMO-CASVB case.

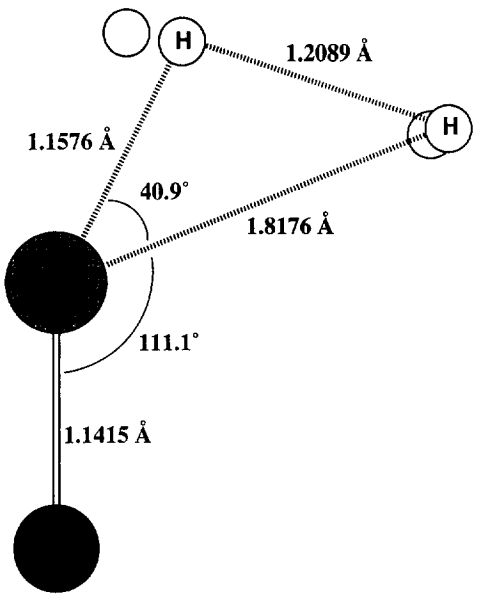

Fig. 17. The structure where the total occupation numbers of the CH bonds and HH bond valence bond structures are equal. The hydrogen atoms not bonded to the carbon atom represent the position at the transition state.

numbers are defined as a measure of bond nature to trace the chemical bonds along the reaction path. The two CASVB methods give a quite similar description for the bond natures during the reactions. We also examined the unimolecular dissociation reaction $H_2CO \rightarrow H_2 + CO$. TS is closer to the reactant H_2CO than to the product $H_2 + CO$. At TS the CH bond character is dominant over the HH bond character. On the intrinsic reaction coordinate of the reaction, the point where the contributions of the two bond characters become equal is 0.42 bohr(amu)$^{1/2}$ after TS, and after that the HH bond character becomes dominant. Generally, the bond formation or dissociation occurs at an early stage or a late stage on the reaction path and the location does not coincide with TS in an asymmetric reaction.

The nature of bond dissociation and formation can be viewed quantitatively by the use of the occupation numbers of VB structures. This analysis is applicable to reactions involving excited states as well as the ground state. We believe that the CASVB occupation number analysis is a useful tool for understanding chemical reaction mechanisms.

Acknowledgements

The present research is supported in part by a Grant-in-Aid for Scientific Research from the Ministry of Education, Science, Sports and Culture of Japan. The CASSCF and CASVB wave functions were obtained by a modified version of HONDO98 (Ref. [36]). The perturbation calculations were carried out with an MR2D program (Refs. [37,38]). The orbital contour maps were plotted using a PLTORB program in GAMESS (Ref. [39]).

References

[1] K. Hirao, H. Nakano, K. Nakayama, M. Dupuis, J. Chem. Phys. 105 (1996) 9227.
[2] K. Hirao, H. Nakano, K. Nakayama, J. Chem. Phys. 107 (1997) 9966.
[3] K. Nakayama, H. Nakano, K. Hirao, Int. J. Quantum Chem. 66 (1998) 157.
[4] Y. Kawashima, K. Nakayama, H. Nakano, K. Hirao, Chem. Phys. Lett. 267 (1997) 82.
[5] J.M. Foster, S.F. Boys, Rev. Mod. Phys. 32 (1960) 300.
[6] K. Ruedenberg, M.W. Schmidt, M.M. Gilbert, S.T. Elbert, Chem. Phys. 71 (1982) 41.
[7] K. Ruedenberg, M.W. Schmidt, M.M. Gilbert, Chem. Phys. 71 (1982) 51.
[8] K. Ruedenberg, M.W. Schmidt, M.M. Gilbert, S.T. Elbert, Chem. Phys. 71 (1982) 65.
[9] T. Thorsteinsson, D.L. Cooper, J. Gerratt, P.B. Karadakov, M. Raimondi, Theor. Chim. Acta 93 (1996) 343.
[10] T. Thorsteinsson, D.L. Cooper, Theor. Chim. Acta 94 (1996) 233.
[11] T. Thorsteinsson, D.L. Cooper, J. Gerratt, M. Raimondi, Theor. Chim. Acta 95 (1997) 131.
[12] B. Liu, J. Chem. Phys. 58 (1973) 1925.
[13] P. Siegbahn, B. Liu, J. Chem. Phys. 68 (1978) 2457.
[14] B. Liu, J. Chem. Phys. 80 (1984) 581.
[15] M.R.A. Blomberg, B. Liu, J. Chem. Phys. 82 (1985) 1050.
[16] K.A. Peterson, D.E. Woon, T.H. Dunning, J. Chem. Phys. 100 (1994) 7410.
[17] D.L. Diedrich, J.B. Anderson, Science 258 (1992) 786.
[18] P. Maitre, J.-M. Lefour, G. Ohanessian, P.C. Hiberty, J. Phys. Chem. 94 (1990) 4082.
[19] P. Maitre, P.C. Hiberty, G. Ohanessian, S.S. Shaik, J. Phys. Chem. 94 (1990) 4089.
[20] T.H. Dunning, J. Chem. Phys. 90 (1989) 1007.

[21] Basis sets were obtained from the Extensible Computational Chemistry Environment Basis Set Database, Version 1.0, as developed and distributed by the Molecular Science Computing Facility, Environmental and Molecular Sciences Laboratory which is part of the Pacific Northwest Laboratory, P.O. Box 999, Richland, Washington 99352, USA, and funded by the US Department of Energy. The Pacific Northwest Laboratory is a multiprogram laboratory operated by Battelle Memorial Institute for the US Department of Energy under contract DE-AC06-76RLO 1830. Contact David Feller, Karen Schuchardt, or Don Jones for further information.
[22] K. Hirao, Chem. Phys. Lett. 190 (1992) 374.
[23] K. Hirao, Chem. Phys. Lett. 196 (1992) 397.
[24] K. Hirao, Chem. Phys. Lett. 201 (1993) 59.
[25] K. Hirao, Int. J. Quantum Chem. S26 (1992) 517.
[26] There are typographical errors in page 9973 in Ref. 2. Occupation numbers in the hydrogen wave functions should be 0.9122 and 0.0878 for the covalent and ionic structures, respectively.
[27] R.L. Jaffe, D.M. Hays, K. Morokuma, J. Chem. Phys. 60 (1974) 5108.
[28] R.L. Jaffe, K. Morokuma, J. Chem. Phys. 64 (1976) 4881.
[29] J.D. Goddard, H.F. Schaefer, J. Chem. Phys. 70 (1979) 5117.
[30] G.F. Adams, G.D. Bent, R.J. Bartlett, G.D. Purvis, J. Chem. Phys. 75 (1981) 834.
[31] J.D. Goddard, Y. Yamaguchi, H.F. Schaefer, J. Chem. Phys. 75 (1981) 3459.
[32] M.J. Frisch, R. Krishnan, J.A. Pople, J. Phys. Chem. 85 (1981) 1467.
[33] G.E. Scuseria, H.F. Schaefer, J. Chem. Phys. 90 (1989) 3629.
[34] M. Dupuis, W.A. Lester, Jr., B.H. Lengsfield, B. Liu, J. Chem. Phys. 79 (1983) 6167.
[35] H. Nakano, K. Nakayama, K. Hirao, M. Dupuis, J. Chem. Phys. 106 (1997) 4912.
[36] M. Dupuis, S. Chin, A. Marquez, in: G.L. Malli (Ed.), Relativistic and Electron Correlation Effects in Molecules and Clusters, NATO ASI Series, Plenum, New York, 1992.
[37] MR2D Ver. 2, H. Nakano, University of Tokyo, 1995.
[38] H. Nakano, J. Chem. Phys. 99 (1993) 9873.
[39] M.W. Schmidt, K.K. Baldridge, J.A. Boatz, S.T. Elbert, M.S. Gordon, J.H. Jensen, S. Koseki, N. Matsunaga, K.A. Nguyen, S. Su, T.L. Windus, M. Dupuis, J.A. Montgomery, J. Comput. Chem. 14 (1993) 1347.